

INFLUENCE OF LAYER STRUCTURE ON PERFORMANCE OF AlGaN/GaN HEMTs

*Peter Benko¹, Jaroslav Kováč¹, Jaroslava Škriniarová¹, Peter Kordoš^{1,2},
Ladislav Harmatha¹*

¹*Institute of Electronics and Photonics, Faculty of Electrical Engineering and Information Technology, Slovak University of Technology, Ilkovičova 3, 812 19 Bratislava, Slovakia*

²*Institute of Electrical Engineering, Slovak Academy of Sciences, Dúbravská cesta 9, 841 04 Bratislava, Slovakia*

E-mail: peter.benko1@stuba.sk

Received 10 May 2012; accepted 15 May 2012.

1. Introduction

Wide bandgap semiconductors are extremely attractive for a large area of electronics industry. Among various materials and device technologies, the AlGaN/GaN high-electron mobility transistor (HEMT) seems to be the most promising. The HEMT transistors are applicable mainly in areas of electronics as power and communications devices [1, 2]. In this paper, we report properties of three different AlGaN/GaN HEMT structures investigated by C - V and I - V measurement.

2. Experiment

The AlGaN/GaN material structures were grown by low-pressure metalorganic vapour phase epitaxy on 4H-SiC and consisted of 1.7 μm thick GaN buffer, Fe doped away from channel followed by 22 nm thick $\text{Al}_{0.26}\text{Ga}_{0.74}\text{N}$ barrier layer (Fig. 1(a)) or 1.25 nm AlN interlayer followed by 20 nm thick $\text{Al}_{0.29}\text{Ga}_{0.71}\text{N}$ barrier layer (Fig. 1(b)) and 1.5 μm thick GaN buffer followed by 25 nm thick $\text{Al}_{0.20}\text{Ga}_{0.80}\text{N}$ barrier layer (Fig. 1(c)). The AlGaN barrier was intentionally undoped. Nb(20 nm)/Ti(20 nm)/Al(100 nm)/Ni(40 nm)/Au(50 nm) metallic system was used to form alloyed ohmic contacts to AlGaN/GaN heterostructure. After optimal rapid thermal annealing (RTA) at 850 $^{\circ}\text{C}$ for 35 s in a nitrogen atmosphere the ohmic contacts exhibit low contact resistivity value. In the next step a MESA isolation was performed using a reactive ion etching (RIE) of AlGaN/GaN in CCl_4 plasma gas. The depth of MESA etching was proposed to be about 100 nm. Electron beam evaporated Ni(40 nm)/Au(100 nm) metallic system in combination with a lift-off technique where used to form the Schottky gate contacts. The expanded contacts consist of Ti(30 nm)/Au(120 nm).

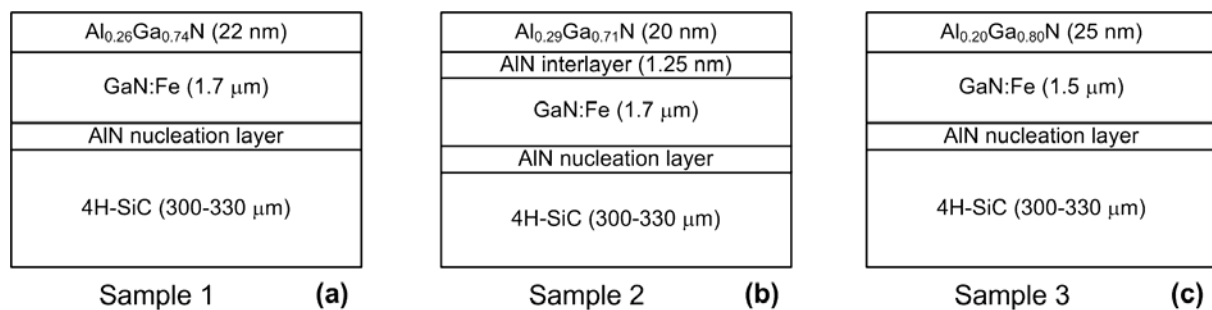


Fig.1: Investigated heterostructures with (a) $\text{Al}_{0.26}\text{Ga}_{0.74}\text{N}$ layer (sample 1), (b) $\text{Al}_{0.29}\text{Ga}_{0.71}\text{N}$ layer (sample 2) and (c) $\text{Al}_{0.20}\text{Ga}_{0.80}\text{N}$ layer (sample 3).

The C - V and I - V characteristics were measured using Hawlet Packard 4280A and Agilent 4155C equipment, respectively.

3. Results and discussion

Fig. 2(a) shows C - V characteristics of the Schottky structures measured on samples 1-3 at the frequency 1 MHz. The thickness of AlGa N barrier layer determined from capacitance at the zero bias is ~ 21 , ~ 21 and ~ 24 nm for samples 1, 2 and 3, respectively. The carrier concentration depth profiles for all samples are shown in Fig. 2(b).

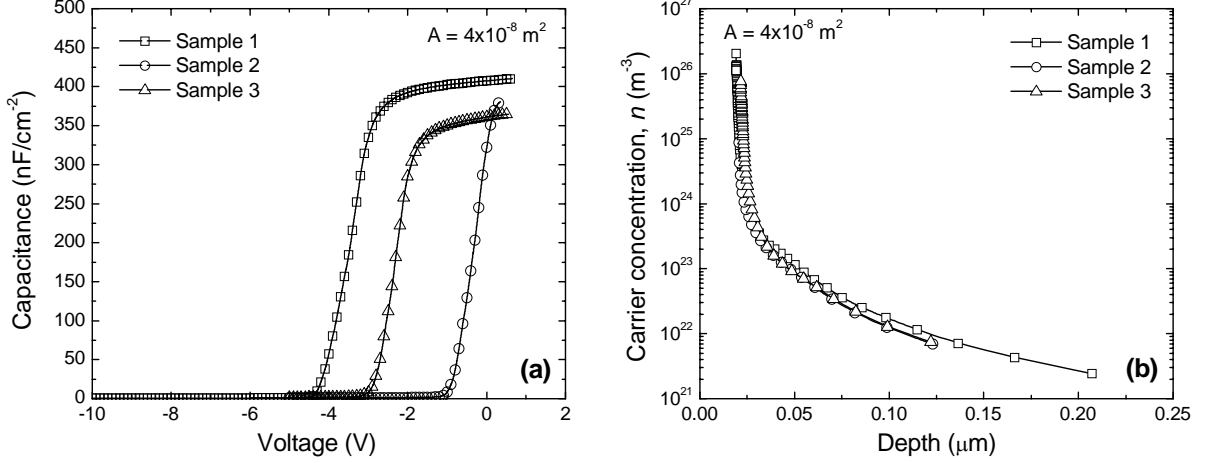


Fig.2: (a) C - V characteristics and (b) plots of carrier concentration vs. depth for various AlGa N /Ga N heterostructures.

The sheet charge density of carriers in channel n_S was evaluated by integration of the C - V characteristics [3] as

$$n_S = \frac{1}{q} \int \frac{C}{A} dV_G, \quad (1)$$

where A is area. For comparison and verification of values n_S we have also determined value of sheet charge density in channel from carrier concentration depth profile as

$$n_S^{n(x)} = \int n dx. \quad (2)$$

Values of n_S and $n_S^{n(x)}$ for all samples are summarized in Tab. 1. Values of n_S evaluated by Eq. (1) are in good agreement with values of $n_S^{n(x)}$ evaluated by Eq. (2). The sample 1 compared to samples 2 and 3 has the highest value of $n_S \sim 1.0 \times 10^{13} \text{ cm}^{-2}$, therefore the high value of saturation drain current I_{DS} is expected for this sample. The sheet charge density, n_S for samples 2 and 3 is $\sim 1.6 \times 10^{12} \text{ cm}^{-2}$ and $\sim 6.3 \times 10^{12} \text{ cm}^{-2}$, respectively. Output and transfer I - V characteristics are shown in Fig. 3, Fig. 4, and Fig. 5. As we expected, the highest value of drain saturation current $I_{DS} = 0.46 \text{ A/mm}$ achieved sample 1. Value of drain saturation current I_{DS} for sample 2 and sample 3 is 0.07 A/mm and 0.25 A/mm , respectively. However, the sample 2 has significantly higher value of the threshold voltage compared to samples 1 and 3.

Tab. 1. Overview of the results of capacitance measurements.

	Sample 1	Sample 2	Sample 3
$n_S \text{ (cm}^{-2}\text{)}$	1.03×10^{13}	1.70×10^{12}	6.34×10^{12}
$n_S^{n(x)} \text{ (cm}^{-2}\text{)}$	1.02×10^{13}	1.53×10^{12}	6.16×10^{12}

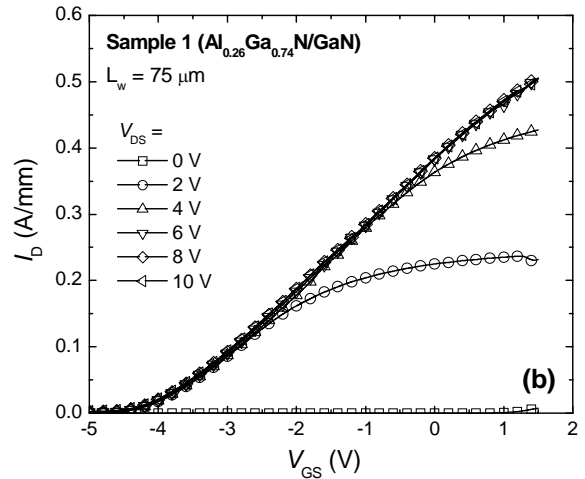
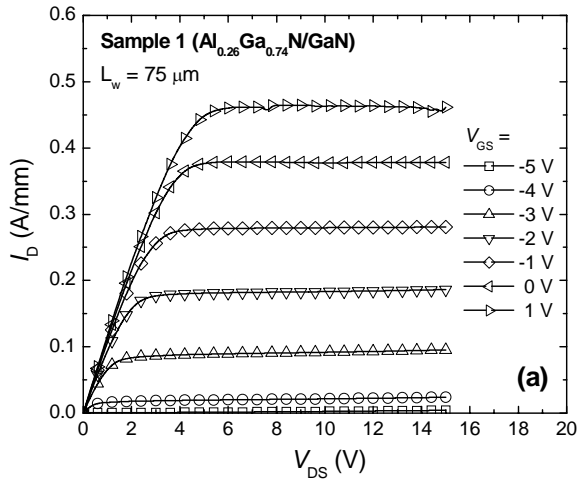


Fig.3: (a) Output I - V characteristics and (b) transfer I - V characteristics of $Al_{0.26}Ga_{0.74}N/GaN$ HEMT.

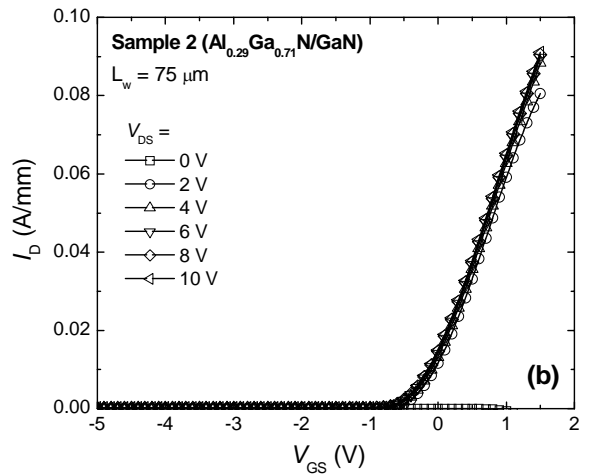
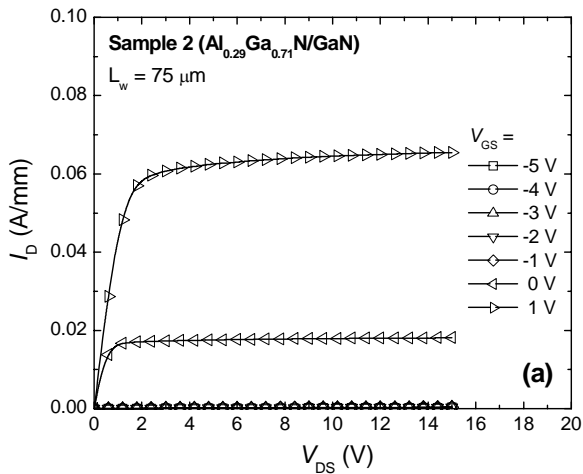


Fig.4: (a) Output I - V characteristics and (b) transfer I - V characteristics of $Al_{0.29}Ga_{0.71}N/GaN$ HEMT with AlN interlayer.

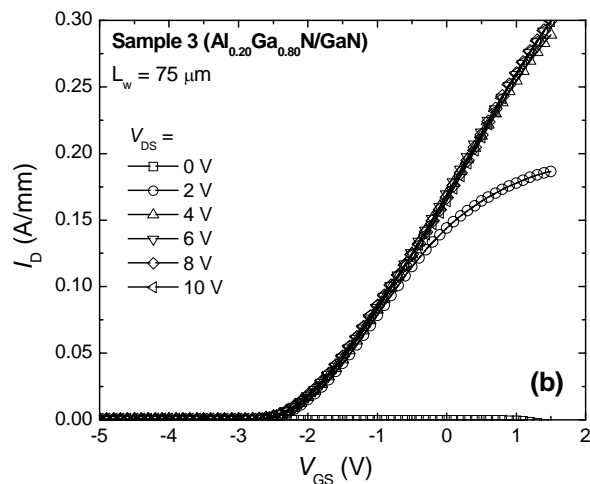
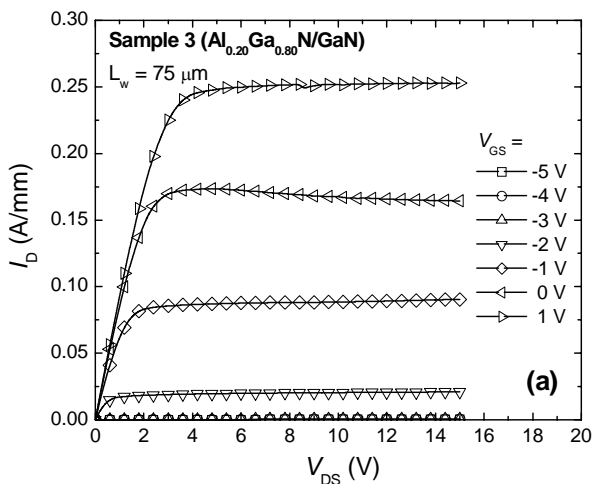


Fig.5: (a) Output I - V characteristics and (b) transfer I - V characteristics of $Al_{0.20}Ga_{0.80}N/GaN$ HEMT.

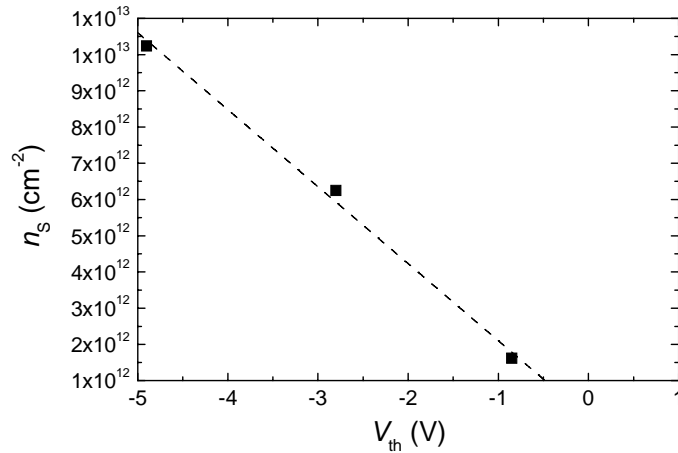


Fig.6: n_s vs. V_{th} plot. Straight lines represent linear least-square fits to the experimental data.

The threshold voltage V_{th} is ~ -4.9 , ~ -0.8 and ~ -2.8 V for samples 1, 2 and 3, respectively. The threshold voltage is given as

$$V_{th} \cong \phi_B - \Delta E_C - \frac{qdn_s}{\varepsilon}, \quad (3)$$

where ϕ_B is Schottky barrier high, ΔE_C is conduction band offset, d is thickness of AlGaIn barrier layer and ε is permittivity. Influence of ε , d and the term $(\phi_B - \Delta E_C)$ upon change of AlGaIn layer composition and thickness on V_{th} (Eq.(3)) is negligible. Hence, the major impact on the threshold voltage has sheet charge density, n_s as we can see in Fig. 6. From this plot can be clearly seen a linear relation between the sheet charge density and the threshold voltage. Therefore, by decreasing sheet charge density in the channel it is possible to reach threshold voltage close to zero. Nevertheless, we must realize that too low value of sheet charge density may leads to significantly low drain saturation current I_{DS} of HEMT.

4. Conclusion

We investigated properties of three type AlGaIn/GaN HEMT structures with different ratio of AlGaIn layer composition and thickness. The best properties have shown sample 1, which achieved relatively high value of the drain saturation current ($I_{DS} = 0.46$ A/mm) and sheet charge density in channel ($n_s \sim 1.03 \times 10^{13}$ cm^{-2}). On the other hand, despite of low value $I_{DS} = 0.07$ A/mm, sample 2 has the highest value of threshold voltage. Such a HEMT with threshold voltage close to zero can be interesting for digital logic application.

In the next work, we want to focus on investigation and determination of traps state density at AlGaIn/GaN interface and its impact on sheet charge density of carriers in channel by multifrequency and stress measurements.

Acknowledgement

The authors would like to thank Mr. T. Lalinský and Mr. G. Vanko for sample preparation. This work was financially supported by grant of Scientific Grant Agency of the Ministry of Education of Slovak Republic and the Slovak Academy of Sciences No.VEGA-1/0689/09 and VEGA-1/0507/09.

References:

- [1] U.K. Mishra, *Proceedings of the IEEE*, **90**, 1022 (2002).
- [2] G. Vanko: AlGaIn/GaN HEMT pre senzorické aplikácie, Bratislava, 2009.
- [3] R. Kreher, *Physica Status Solidi A*, **135**, 597, 1993